

Image Morphological Reconstruction Using Dehazing Algorithm

¹SYED SAMEER AHMED, ²MD ASIM IQBAL, ³K RAJESH REDDY

ABSTRACT:

Outside pictures are utilized in countless applications, for example, observation, distant detecting, and independent route. The best issue with these kinds of pictures is the impact of ecological contamination: fog, exhaust cloud, and haze beginning from suspended particles noticeable all around, for example, residue, carbon and water drops, which cause corruption to the picture. The end of this sort of debasement is basic for the contribution of PC vision frameworks. The greater part of the best in class research in dehazing calculations is centered around improving the assessment of transmission maps, which are otherwise called profundity maps. The transmission maps are important in light of the fact that they have an immediate connection to the nature of the picture rebuilding. In this paper, a novel rebuilding calculation is proposed utilizing a solitary picture to diminish the natural contamination impacts, and it depends on the dim channel earlier and the utilization of morphological remaking for the quick figuring of transmission maps. The acquired exploratory outcomes are assessed and contrasted subjectively and quantitatively and other dehazing calculations utilizing the measurements of the Peak Signal-to-Noise Ratio (PSNR) and Structural Similarity (SSIM) list; in view of these measurements, it is discovered that the proposed calculation has improved execution contrasted with as of late presented approaches.

Keywords: dehazing Algorithm, Structural Similarity (SSIM), Peak Signal-to-Noise Ratio (PSNR)

I. INTRODUCTION

Outside pictures are presented to unfriendly climate conditions, for example, cloudiness, mist or brown haze, which cause impacts, for example, scene obscuring, contrast debasement, and shading change, among others. Cloudiness is among the most well-known air conditions and is brought about by coasting particles, for example, water drops or whatever other airborne that mirrors the light, diffusing it noticeable all around and diminishing the perceivability of subtleties. Vision frameworks applied to distant detecting, reconnaissance, and autonomous route for the most part use input pictures under antagonistic climate conditions; subsequently, the outcomes created rely upon the nature of the picture got as info. Air dispersing includes nonlinear and information subordinate clamor to

¹M.Tech Student, Department of ECE, KU College of Engineering & Technology, Kakatiya University, Warangal, Telangana, India.

²Asst. Professor of ECE, Kakatiya University, Warangal, Telangana, India.

³Assi Academic Consultant of ECE, Kakatiya University, Warangal, Telangana, India

the caught open air picture, which makes picture reclamation a troublesome cycle; therefore, a few examination works have zeroed in on reducing the dimness impacts in pictures caught utilizing vision frameworks by planning and applying debasing calculations [1], which can be partitioned into those requiring extra data from the scene (for example, in [2], a strategy for cloudiness expulsion that uses the relationships between's dim pictures and murkiness free pictures as outer data is introduced) and those utilizing one single picture (in [3], an investigation and assessment of existing single-picture debasing calculations, utilizing a huge scope benchmark of engineered and certifiable dim pictures, is introduced). The calculations that utilization a solitary picture to reduce the impacts of unfavorable barometrical conditions are the most considered these days since they are helpful for down to earth applications, for example, self-sufficient vehicle route, reconnaissance and far off detecting [4], [5]. In such manner, dull channel earlier (DCP), which comprises of assessing the transmission guide of a picture by assessing the profundity of every component in it, has been utilized in blend with different calculations for quick calculation of exact transmission maps [6], at the expense of long calculation times bargaining its usage on online vision frameworks. Along these lines, ongoing examination has zeroed in on the calculation speed of transmission maps, expecting to protect the picture quality.

In this work, a novel quick calculation is proposed for reducing cloudiness impacts utilizing morphological recreation to safeguard significant structures in the entirety of its stages and refine the transmission-map calculation of single pictures caught by vision frameworks, making it practical for use in online applications.

The rest of the composition is sorted out as follows. Segment II gives a short writing audit of related work. Segment III presents a review of the hypothetical foundation used in this work. Area IV depicts the proposed method and its execution top to bottom. Gotten results are introduced in Section V and thought about against those acquired from six distinctive debasing calculations. At last, ends are given in Section VI.

II. RELATED WORK

As depicted previously, debasing calculations can be isolated into two gatherings. Among those requiring extra data are the accompanying. In [7], a debasing technique is proposed utilizing an obvious picture with a close infrared picture of the same scene to get a debased shading picture. In [8], system for perusing, improving, and controlling casual outdoor photos is presented by joining them with preexisting geo-referenced computerized territory and metropolitan models. Other works gauge the caught scene profundity utilizing multiple pictures taken under various climate conditions [9],[10]. A few calculations eliminate fog by exploiting of light polarization [11], [12]. In any case, their principle burden is that the necessities are not generally accessible or are difficult to follow. For instance, the infrared algorithm requires a changed camera to get the infrared information. It is worth mentioning that calculations requiring various pictures are hard to actualize for online applications [9], whereas algorithms that utilization pictures with various degrees of polarization are delicate to vibrations or development [10].

Calculations utilizing a solitary picture to reduce dimness effects are among the most important exploration. In [13], fog is removed by expanding neighborhood contrast in the examined picture. It was seen that a cloudiness free picture ought to have higher differentiation than a hazed picture. In [14], autonomous part analysis(ICA) is utilized to address fog by assessing the albino in the captured scene and the spread medium, whereas transmission and concealing of the surface are connected locally. In [15], a transmission map is acquired by examining the optical model and reworking the underlying transmission map under an extra limit earlier. In [16], DCP is proposed for assessing the picture transmission map, which comprises of estimating every component's profundity in the picture, and it inessential for reestablishing it. The introduced outcomes are agreeable; regardless, the transmission map produces radiances around the reestablished picture edges. To improve their calculation, the authors introduced delicate tangling for cleaning the transmission map, sacrificing calculation time and risking its usage infest picture handling frameworks for online applications. Consequently, DCP has been utilized in mix with other algorithms, searching for quick calculation of accurate transmission maps [6]. For instance, in [17], climatic dissipating and DCP hypotheses are utilized for single-imaged hazing. A transmission map is assessed utilizing a fast average channel, the locale projection strategy is embraced to obtain the air light, and picture shading remuneration is implemented utilizing the Weber-Fechner Law. In [18], a median filter is incorporated for eliminating coronas from a picture. In [19], a respective channel and a transmission channel are utilized for removing noise while safeguarding the edges, and the transmission map is refined to recoup the scene. In [20], an amendment of white parity is acquainted in DCP with improve the picture quality by obtaining two parts: the mirrored light in the picture and the light from the climate. In [21], a segmentation algorithm called mean move sifting is proposed for refining the transmission map created by DCP to improve there constructed picture. In [22], a combination based transmission estimation is presented, joining the combination weighting plan and the barometrical light figured from the Gaussian-based dim channel technique. In [23], a direct shading constriction earlier is proposed dependent on the distinction between the pixel splendor and immersion in cloudy pictures. In [24], a pixel-put together calculation depending with respect to a nonlocal earlier and the presumption that a dimness free picture can be dependably spoken to with only a couple hundred unmistakable tones is proposed.

From the explored work in ongoing writing, unmistakably present exploration on reducing fog impacts in pictures centers around improving the speed of transmission map calculation for the first DCP procedure [16], [25], without losing the picture quality [15]; in any case, these calculations have just accomplished halfway upgrades [1], [5]. The commitment of this work is a novel quick calculation for lessening dimness impacts, utilizing morphological remaking in the entirety of its stages to refine the transmission map calculation of single pictures caught by a dream framework, making it doable for online applications. The proposed strategy depends on the DCP procedure and to the best of the creators' information, the presented approach, which radically decreases handling time, has never been utilized for this reason. In such manner, the procedure proposed in this paper is in any event two significant degrees quicker than the first DCP calculation. Furthermore, obtained subjective and quantitative outcomes utilizing the Peak Signal-to-Noise Ratio(PSNR) and the Structural Similarity (SSIM) file show that the proposed strategy accomplishes preferred outcomes over other as of late presented cutting edge calculations for this subject.

III. BACKGROUND

1. Atmospheric dissipating model

Fig. 1 portrays how a scene may be influenced by ecological contamination delivering dimness in the caught picture. Its comparing numerical model is depicted by (1) [26].

$$I(\chi) = J(\chi)t(\chi) + A(1-t(\chi)) \quad (1)$$

In (1), $I(\chi)$ is the watched force in each channel, R, G and B (RGB), of the pixel $\chi=(x, y)$ in the caught scene by a camera. $J(\chi)$ is the vector force of the scene's unique zone in reality that compares to the pixel $\chi=(x, y)$. A is the color vector of the worldwide environmental light. $t(\chi)$ is known as the transmission, which depicts the part of light that isn't dissipated or ingested and arrives at the camera. Under a homogeneous air condition, the transmission $t(\chi)$ can be communicated by (2).

$$t(\chi) = e^{-\beta d(\chi)} \quad (2)$$

where β is the environment dispersing coefficient and $d(\chi)$ is the profundity of the component χ ; hence, a guide of transmission is proportional to a profundity map. The primary trouble in obtaining $t(\chi)$ settles upon the way that, when a picture is caught, A and $t(\chi)$ in (1) are obscure. In this manner, the utilization of priors and some assumptions are important to discover an estimation of $J(\chi)$. The unique calculation, which depends on DCP and was proposed in [16], makes it conceivable to lead an accurate estimation of A and $t(\chi)$, yet at a high computational cost. Hence, it is important to search for an elective strategy ready to furnish palatable outcomes with less handling time.

M. Dark channel earlier (DCP)

DCP is a measurable perception of what occurs in pictures that don't present the issue of fog and are gained in outside conditions. For the vast majority of the patches in a picture that don't speak to the sky, there is in any event a low-force pixel in each shading channel (R, G or B). Consequently, the negligible force of one pixel in such fixes has an incentive almost 0 [16]. For a picture $I(\chi)$, the dull channel $I^{dark}(\chi)$ is characterized by (3)[16].

$$I^{dark}(\chi) = \min_{C \in \{R, G, B\}} \left(\min_{y \in \Omega(\chi)} (I^C(y)) \right) \quad (3)$$

where $\Omega(\chi)$ is the fix focused in χ , I^C is the shading channel C (i.e., R, G, or B) from I , and y is the pixel contained in $\Omega(\chi)$.

$$I^{dark}(\chi) \rightarrow 0 \quad (4)$$

Consequently, DCP is communicated by (4).

In [16], the calculation appeared in Fig. 2 is proposed to dehazean picture I, of tallness h and width w pixels, utilizing DCP. The calculation produces brilliant outcomes, yet its primary downside is its computational multifaceted nature; consequently, in this work, a procedure to debase a picture is proposed by consolidating DCP with morphological remaking to improve the calculation speed for the transmission map estimation N.

Morphological reproduction

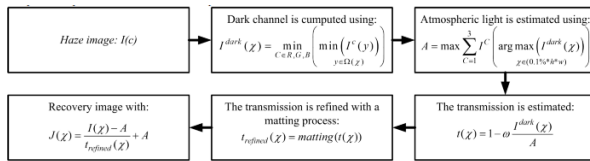


Fig. 2. Dehazing algorithm proposed in [16].

The morphological reproduction depends on numerical morphology activities, and it is utilized to improve pictures and safeguard principle highlights as article shapes. The proposed calculation utilizes the ideas of opening and shutting for picture remaking, which depend on strategies, for example, dim scale disintegration, dim scale expansion, geodesic disintegration and widening, and reproduction by disintegration and enlargement, considering a dim scale picture I, a level organizing component S with a subjective shape framed by pixels s, and the position (x, y) of the pixel χ in the picture I.

Grayscale disintegration

The disintegration of I by S is characterized as the base estimation of the picture in the coordinating locale with s when the source is engaged at the position $\chi=(x, y)$ [27], as depicted in (5)

$$[\varepsilon_B(I)](\chi) = \min_{s \in S} I(\chi + s) \tag{5}$$

Grayscale widening

The widening δ_B of I by S is characterized as the greatest estimation of the picture in the window characterized by the birthplace of S when S is at $\chi=(x, y)$, and it is communicated by (6)

$$[\delta_B(I)](\chi) = \max_{s \in S} I(\chi + s) \tag{6}$$

Morphological remaking

A morphological remaking is communicated as far as geodesic enlargement and geodesic disintegration.

Geodesic Dilation

In dark scale pictures, the size-1 geodesic expansion $\delta_g(1)$ of I(marker picture) as for F (veil picture) is characterized by

$$\delta_g^{(1)}(I) = \delta^{(1)}(I) \wedge F \tag{7}$$

where I and F are a similar size, the force connection $I \leq F$ holds for all pixels in the pictures, and \wedge is the operator minimum. Thus, the n-size geodesic expansion $\delta_g(n)$ is as given in (8).

$$\delta_g^{(n)}(I) = \delta_g^{(1)}[\delta_g^{(n-1)}(I)] \tag{8}$$

with $\delta_g(0)(I) = I$

Geodesic Erosion

In dim scale pictures, the size-1 geodesic disintegration $\varepsilon_g(1)$ of I(marker picture) concerning G (the veil picture) is characterized by

$$\varepsilon_g^{(1)}(I) = \varepsilon^{(1)}(I) \vee G \tag{9}$$

where I and F are a similar size, the power connection $I \geq F$ holds for all pixels in the pictures, and \vee is the administrator most extreme. The n-size geodesic disintegration is appeared in (10)

$$\varepsilon_g^{(n)}(I) = \varepsilon_g^{(1)}[\varepsilon_g^{(n-1)}(I)], \text{ where } \varepsilon_g^{(0)}(I) = I. \tag{10}$$

Reconstruction by enlargement

Reproduction by widening is acquired through the geodesic expansion of marker I on the veil F, emphasizing until security is reached, and it is meant by $R_g\delta(I)$ as appeared in (11).

$$R_g^\delta(I) = R_g^{(i)}(I) \tag{11}$$

Reconstruction by disintegration

Remaking by disintegration is acquired through the geodesic disintegration of marker I on the cover G, repeating until security is reached. It is indicated by as appeared in (12).

$$R_g^\varepsilon(I) = \varepsilon_g^{(i)}(I) \tag{12}$$

$$\varepsilon_g^{(i)}(I) = \varepsilon_g^{(i+1)}(I).$$

Soundness is accomplished when

Opening and shutting by remarking

Opening and shutting by remarking reestablish the types of articles that the organizing component surpasses after each cycle. The recreation accuracy relies upon the closeness of the organizing component to the state of the items. The n-size opening by remarking of a picture I is depicted by (13).

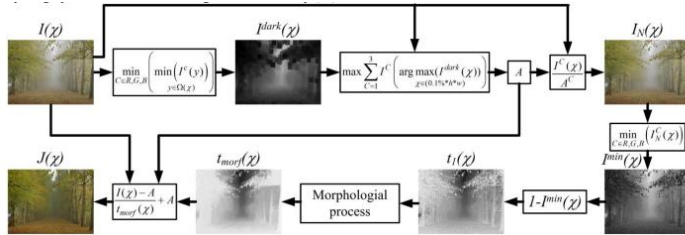


Fig. 3. Flowchart of the proposed algorithm.

Analogously, closing by reconstruction is defined in equation (14).

$$\gamma_R^{(n)}(I) = R_I^\delta[\varepsilon^{(n)}(I)] \quad (13)$$

$$\phi_R^{(n)}(I) = R_I^\varepsilon[\delta^{(n)}(I)] \quad (14)$$

IV. THE PROPOSED ALGORITHM

The dull direct depicted in (3) can be expressed regarding a morphological disintegration as:

$$I^{dark}(\chi) = \left[\varepsilon_S \left(\min_{C=R,G,B} (I^C(y)) \right) \right](\chi) \quad (15)$$

In light of (15), a morphological strategy that can yield a picture without murkiness or coronas is proposed as portrayed in Fig. 3, and it is portrayed as follows:

Thinking about $I(\chi)$ as a RGB picture of tallness h and width w pixels, where each pixel position is given by $\chi=(x, y)$, the dim channel $I^{dark}(\chi)$ is processed from $I(\chi)$ as indicated by (15), with the climatic light A given by

$$A = \max_{C=1}^3 \left(I^C \left(\arg \max_{\chi \in (0.1\%*h*w)} (I^{dark}(\chi)) \right) \right) \quad (16)$$

The picture $I(\chi)$ is standardized concerning the air light A to acquire dull channel esteems somewhere in the range of zero and one, as given by

$$I_N(\chi) = \frac{I(\chi)}{A} \quad (17)$$

The negligible channel is characterized as:

$$I^{\min}(\chi) = \min_{C=R,G,B} (I_N^C(y)) \quad (18)$$

The underlying transmission map is figured as:

$$t_1(\chi) = 1 - I^{\min}(\chi) \quad (19)$$

Fig. 4 shows each phase of the proposed morphologic cycle utilized for refining the underlying transmission, which utilizes a square organizing component S .

$$t_2(\chi) = \phi_R^1(t_1(\chi)) \quad (20)$$

In the main stage, an end by recreation is proceeded as:

$$t_3(\chi) = \gamma_R^1(t_2(\chi)) \quad (21)$$

This activity eliminates little dull components over the picture organizing component.

$$R(\chi) = t_1(\chi) - t_3(\chi) \quad (22)$$

An opening by remaking is completed later as:

$$t'_3(\chi) = t_3(\chi) - \min(t_3(\chi)) \left(\frac{\max(t_1(\chi)) - \min(t_1(\chi))}{\max(t_3(\chi)) - \min(t_3(\chi))} \right) + \min(t_1(\chi)) \quad (23)$$

This strategy erases little items that are more clear than the climate, and its size is more modest than that of S . These articles are spared by

$$t_{\text{morf}}(\chi) = t'_3(\chi) + R(\chi) \quad (24)$$

To recuperate the scope of qualities for the first transmission, the time periods) are changed to the time spans), and the outcome is spared in $t_3'(x)$, as appeared by:

$$J(\chi) = \frac{I(\chi) - A}{t_{\text{morf}}(\chi)} + A \quad (25)$$

The refined transmission $t_{\text{morf}}(\chi)$ is recouped through:

At long last, the transmission map $t_{\text{morf}}(\chi)$ and the climatic light A_n are applied to the dissipating model to recover the $\text{ImageJ}(\chi)$ without dimness, as appeared by

V. RESULTS

The proposed calculation's viability is surveyed in this part through experimentation. The acquired outcomes are analyzed subjectively and quantitatively against those from various methodologies in late writing. The pictures utilized for approving the proposed strategy were taken from [28] and [29]. A 15-pixel, square organizing component B was utilized during the experimentation. The proposed calculation was actualized on an Intel i5-3320 chip at 2.6 GHz using MATLAB.

Qualitative examination

Fig. 6 shows genuine world external pictures influenced by cloudiness that are prepared through various cutting edge draws near,

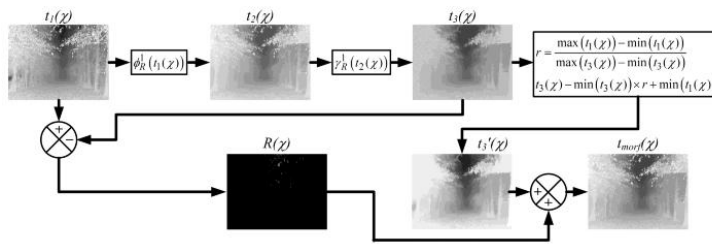


Fig. 4. Morphological cycle.

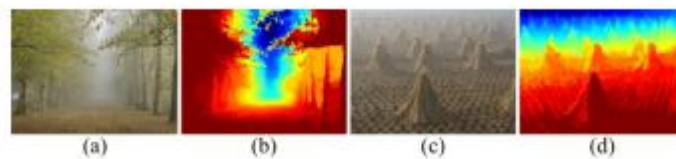


Fig. 5. Instances of transmission maps produced by the proposed calculation, where (a) (c) are the info pictures and (b) (d) are the individual transmission maps.

for example, He et al. [15] (2017), (c) Tarel et al. [18] (2009), (d) Gibson et al. [30] (2013), (e) Kim et al [31] (2013), (f) Zhu et al. [23] (2015), (g) Berman et al. [24] (2016), and the proposed approach in this work, to do a subjective examination of the debased pictures acquired through each. He et all's. procedure and the proposed technique produce a satisfactory picture reclamation, subjectively, since no noticeable deformities are watched. The got outcomes from applying Tare let all's. approach give a few curios in the reestablished pictures (Fig. 6c). The tone is noticeably influenced in the yield pictures (Fig. 6d) from applying Gibson et all's. strategy. The Kim et al.

also, Zhu et al. plans present slight coronas in their recouped pictures (Fig. 6e and Fig. 6f, separately). At last, Berman et all's. technique creates leaves with no homogeneous shading in the acquired pictures (Fig. 6g).

Quantitative examination

Fig. 7 shows eleven pictures utilized for mathematical investigation of the proposed strategy's presentation contrasted with other best in class approaches in the surveyed writing. These pictures have various attributes, and they are debased with fog reenacted by utilizing the model of barometrical dissipating considering the air light vector [0.92, 0.95, 1] as in [29]; they are then treated during experimentation with the calculations of He et al. [15], Tarel et al. [18], Gibson et al.[30], Kim et al. [31], Zhu et al. [23], and Berman et al. [24], just as the methodology proposed in this work. The measurements utilized for quantitatively assessing the proposed calculation's exhibition against that of past methodologies in the checked on writing are the pinnacle signal-to-commotion proportion (PSNR) and the auxiliary comparability (SSIM) file (27) [32].

PSNR is the extent between the greatest conceivable intensity of a picture and the intensity of undermining commotion that influences the devotion of its portrayal. Given a cloudiness free picture $I_{HF}(x)$ and the relating mean square blunder (MSE) among $I_{HF}(x)$ and its reestablished guess $J(x)$, the PSNR is characterized by

$$PSNR = 10 \log_{10} \left[\frac{MAX_{I_{HF}}^2(x)}{MSE} \right] \quad (26)$$

where $MAX_{I_{HF}}^2(x)$ is the squared greatest conceivable pixel estimation of the picture $I_{HF}(x)$, and the comparing MSE is givenas:

$$MSE = \frac{1}{(w \times h)} \sum_{x=1}^w \sum_{y=1}^h (J(x) - I_{HF}(x))^2 \quad (27)$$

with x speaking to the pixel position (x, y) in the picture, with width and stature w and h, separately. The higher the PSNR esteem, the better the picture guess $J(x)$.

The SSIM record is utilized to quantify the similitude between two pictures, and it thinks about three perspectives in reestablished pictures: lighting $l(x)$, contrast $c(x)$, and structure $s(x)$.

$$SSIM(x) = f(l(x), c(x), s(x)) \quad (28)$$

The SSIM list is a decimal incentive between - 1 and 1. SSIM= 1 just when two pictures with indistinguishable arrangements of information are looked at.

Table I and Table II show the PSNR and SSIM record measurements, separately, acquired from each applied methodology, and they quantitatively exhibit the presentation prevalence of the proposed strategy against recently presented approaches for picture debasing rebuilding.

F. Time execution investigation

Table III presents a period utilization correlation of the proposed strategy against cutting edge calculations in the audited writing. This table incorporates data with respect to the treated picture's size in pixels. A 2.6-GHz, 64-digit Intel Core i5-3320 with 12 GB of RAM was utilized under the Windows 10

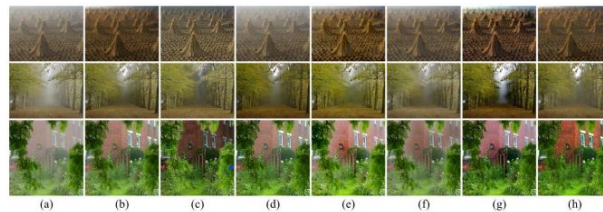


Fig. 6. Correlation of recuperated outside certifiable scenes without murkiness. (a) input pictures, the outcomes from (b) He et al. [15], (c) Tarel et al. [18], (d) Gibson et al. [30], (e) Kim et al [31], (f) Zhu et al. [23], (g) Berman et al. [24], and (h) proposed calculation.

working framework to execute the calculations in MATLAB 2018a. From this table, it is significant that the proposed approach accomplishes quicker preparing time than some other strategy in the assessed writing, from one up to four significant degrees. In such manner, it is imperative to call attention to that, despite the fact that the methodology in He et al. [15] acquires higher rebuilding measurements (PSNR and SSIM), the strategy presented in this work is at any rate three significant degrees quicker than it. Then again, the rebuilding acquired from the presented strategy is quantitatively unrivaled (PSNR y SSIM) and in any event one significant degree quicker than the picture reclamation from all outstanding methodologies in the assessed writing.

Table IV presents a pinnacle memory-utilization examination of the proposed calculation against those equivalent methodologies in Table III. From Table IV, it is significant that the proposed approach has lower memory use than the wide range of various thought about methods, then again, actually from Gibson et al. [30], for certain cases. Nonetheless, the proposed strategy outperforms that from Gibson et al. as to picture reproduction execution and time utilization by in any event one significant degree.

VI. Conclusion

Outside pictures are presented to unfriendly climate conditions, for example, murkiness, which decreases the deceivability of subtleties in a caught scene. Henceforth, a few exploration works have zeroed in on lessening fog impacts in pictures by planning and applying debasing calculations. In such manner, a large portion of the as of

late proposed calculations consolidate DCP with various strategies that search for quick calculation of exact transmission maps, expecting to save the picture quality at the expense of long calculation times. Hence, in this work, a novel quick calculation for decreasing cloudiness impacts utilizing DCP and a recently presented approach was thought about subjectively and quantitatively against best in class strategies; morphological recreation is used to save significant structures

TABLE I
 OBTAINED RESULTS FROM PSNR ANALYSIS

Images	He et al. [15]	Tarel et al. [18]	Gibson et al. [30]	Kim et al. [31]	Zhu et al. [23]	Berman et al. [24]	Proposed algorithm
Bikes1	20.7	8.3	15.5	16.2	12.7	26.1	17.4
Roof62	12.9	11.8	14.0	19.2	13.8	16.0	14.3
Trees2	18.9	16.1	17.4	15.0	18.9	18.5	18.0
Church	19.1	17.2	17.8	18.7	17.2	16.6	18.4
Couch	19.9	15.9	20.8	19.1	18.8	12.3	19.1
Dolls	18.7	16.9	18.6	19.1	21.1	11.9	18.8
Flower1	20.1	16.5	17.0	18.9	18.0	17.4	19.4
Flower2	14.8	14.1	15.4	18.2	18.5	15.1	14.7
Mansion	18.7	16.0	19.1	17.7	20.5	18.2	18.7
Moebius	21.9	11.6	17.5	13.0	15.4	21.0	20.8
Raindeer	19.6	10.7	16.6	12.0	13.3	20.8	18.3
Average	18.7	14.1	17.3	17.0	17.1	17.6	18.0

TABLE III
 COMPUTATIONAL TIME ANALYSIS (SECONDS).

Method	Image Size (pixels)			
	600×400	800×600	1280×720	1920×1080
He et al. [15]	23.35	47.76	97.10	420.98
Tarel et al. [18]	8.13	24.96	111.64	520.02
Gibson et al. [30]	1.19	2.35	4.57	10.43
Kim et al. [31]	0.2	0.3	0.7	1.6
Zhu et al. [23]	0,74	1,31	2,48	5,55
Berman et al. [24]	1,24	2,46	5,12	12,58
Proposed algorithm	0.02	0.04	0.06	0.14

TABLE IV
 MEMORY UTILIZATION (MEGABYTES).

Method	Image Size (pixels)			
	600×400	800×600	1280×720	1920×1080
He et al. [15]	895.5	1792.5	3472.9	8079.9
Tarel et al. [18]	40.3	82.3	159.7	358.7
Gibson et al. [30]	9.3	18.4	70.3	101.2
Kim et al. [31]	53.3	116.3	215.4	468.7
Zhu et al. [23]	16.6	33.1	63.6	142.7
Berman et al. [24]	117.2	234.5	449.9	1012.5
Proposed algorithm	13.0	23.1	43.6	90.3

of the image in all stages. The reviewed literature about the subject involves image reconstruction performance (utilizing PSNR and SSIM index), computation time and memory utilization. From the obtained results, the performance superiority of the proposed method for diminishing haze effects during image reconstruction is clear, as is its high speed processing time that surpasses all other techniques in the reviewed literature from one to four orders of magnitude with less memory utilization. Therefore, the proposed methodology for image dehazing introduced in this work offers a fast, high performance dehazing technique suitable for online vision system applications.

Future work will be directed to improve the proposed algorithm's performance in handling sky regions due to DCP limitations.



Fig. 7. Comparison of recovered scenes without haze. (a) Ground-truth images, (b) input images, the results from (c) He et al. [15], (d) Tarel et al. [18], (e) Gibson et al. [30], (f) Kim et al. [31], (g) Zhu et al. [23], (h) Berman et al. [24], and (i) the proposed algorithm.

REFERENCES

- [1] C. Chengtao, Z. Qiuyu, L. Yanhua, "A Survey of Image Dehazing Approaches," in Proc. Control and Decision Conference (CCDC), Qingdao, China, 2015, pp. 3964–3969.
- [2] F. Yuan, H. Huang, "Picture Haze Removal through Reference Retrieval and Scene Prior," IEEE Trans. Picture Process. vol. 27, no. 9, pp. 4395–4409, Sep. 2018.
- [3] B. Li, W. Ren, D. Fu, D. Tao, D. Feng, W. Zeng, Z. Wang, "Benchmarking Single-Image Dehazing and Beyond", IEEE Trans. Picture Process. vol. 28, no. 1, pp. 492–505, Jan. 2019.
- [4] K. B. Gibson, D. T. Vo, T. Q. Nguyen, "An Investigation of Dehazing Effects on Image and Video Coding," IEEE Trans. Picture Process. vol. 21, no. 2, pp. 662–673, Feb. 2012.
- [5] V. Sahu, M. Singh, "A Survey Paper on Single Image Dehazing," International Journal on Recent and Innovation Trends in Computing and Communication, vol. 3, no. 2, pp. 85–88, Feb. 2015.
- [6] Y.- H. Lai, Y.- L. Chen, C.- J. Chiou, C.- T. Hsu, "Single-Image Dehazing via Optimal Transmission Map Under Scene Priors," IEEE Trans. Circuits Syst. Video Technol., vol. 25, no. 1, pp. 1–14, Jan. 2015.
- [7] L. Schaul, C. Fredembach, S. Susstrunk, "Shading Image Dehazing Using the Near-Infrared," in Proc. sixteenth IEEE International Conference on Image Processing (ICIP), Cairo, Egypt, 2009, pp. 1629–1632.
- [8] J. Kopf, B. Neubert, B. Chen, M. Cohen, D. Cohen-Or, O. Deussen, M. Uyttendaele, D. Lischinski, "Deep Photo: Model-based Photograph Enhancement and Viewing," ACM Trans. Comput. Graph., vol. 27, no. 5, p. 116:1–116:10, Dec. 2008.
- [9] P. Carr, R. Hartley, "Improved Single Image Dehazing Using Geometry," in Proc. Advanced Image Computing: Techniques and Applications (DICTA), Melbourne, VIC, Australia, 2009, pp. 103–110.
- [10] Y. Y. Schechner, S. G. Narasimhan, S. K. Nayar, "Moment Dehazing of Images Using Polarization," in Proc. IEEE Computer Society Conference on Computer Vision and Pattern Recognition (CVPR), Kauai, HI, USA, 2001, p. I-325–I-332.